Jet Propulsion Laboratory
California Institute of Technology

Verification, Validation, and Uncertainty Quantification (VVUQ) for Global Imaging Spectroscopy

David R. Thompson*
Amy Braverman
Kerry Cawse-Nicholson
Michael Gunson
Robert O. Green
Jonathan Hobbs
Charles E. Miller
Michael Turmon

Jet Propulsion Laboratory, California Institute of Technology
*david.r.thompson@jpl.nasa.gov

Copyright 2018 California Institute of Technology. All Rights Reserved. US Government Support Acknowledged.

Agenda

- Motivation and Elements of VVUQ
- Example: The OCO-2 Mission
- VVUQ for imaging spectroscopy
- UQ for requirements definition

Elements of VVUQ

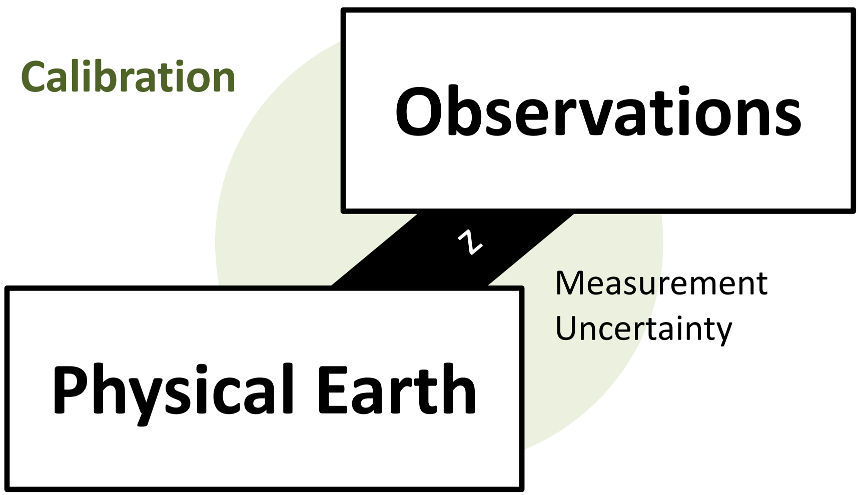

Elements of VVUQ

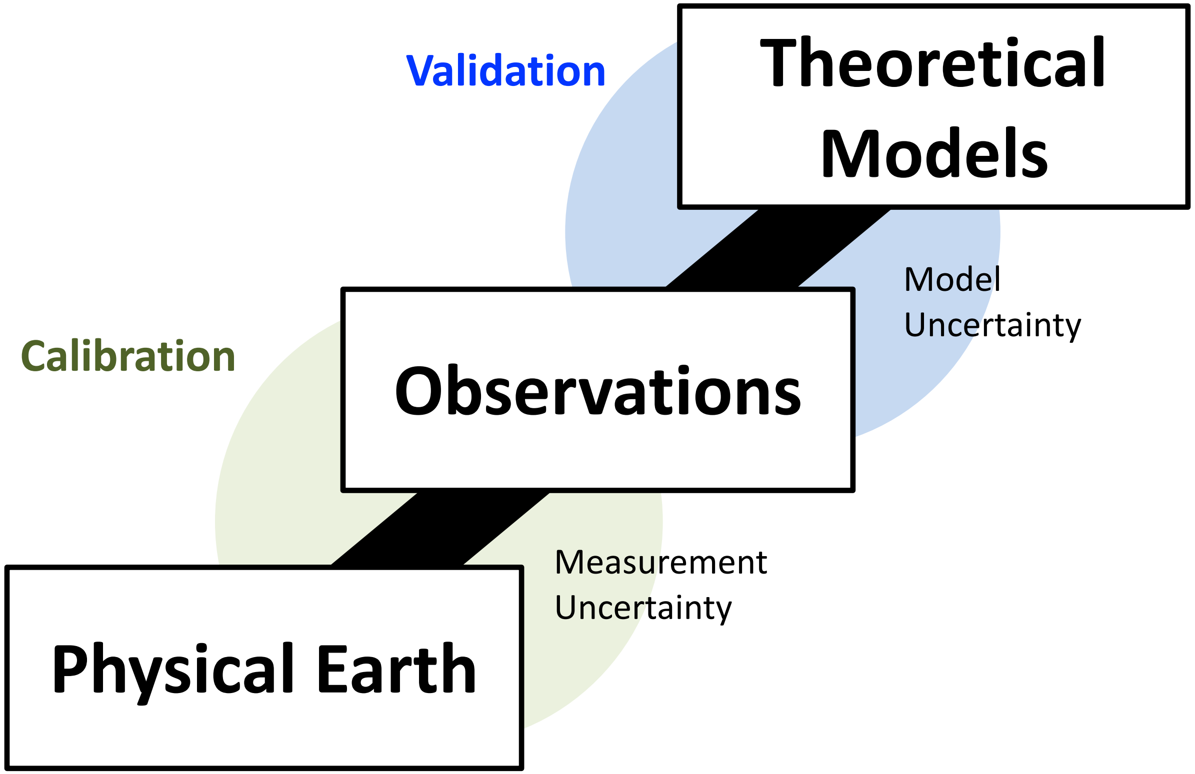

david.r.thompson@jpl.nasa.gov

Elements of VVUQ

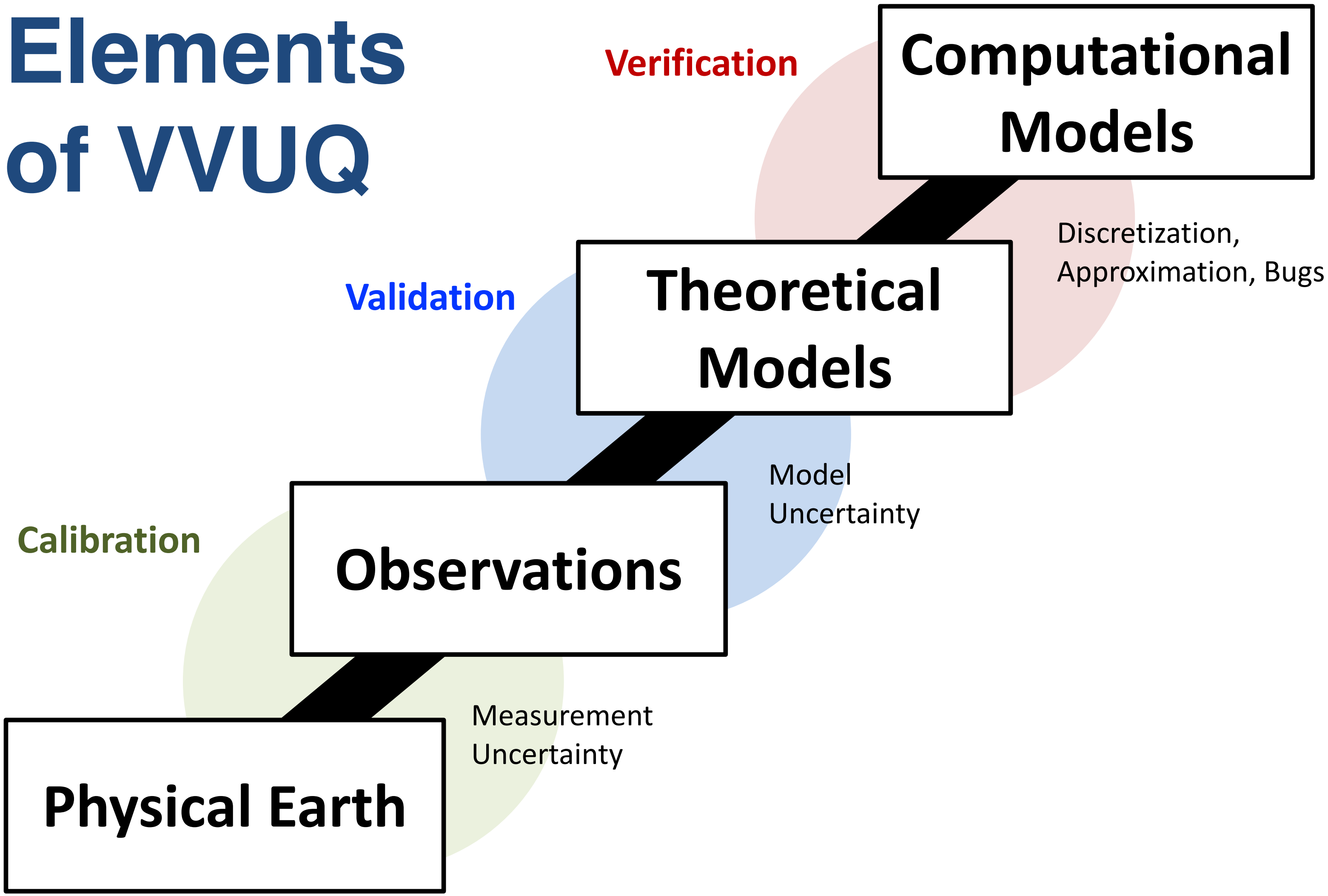

david.r.thompson@jpl.nasa.gov

Elements of VVUQ

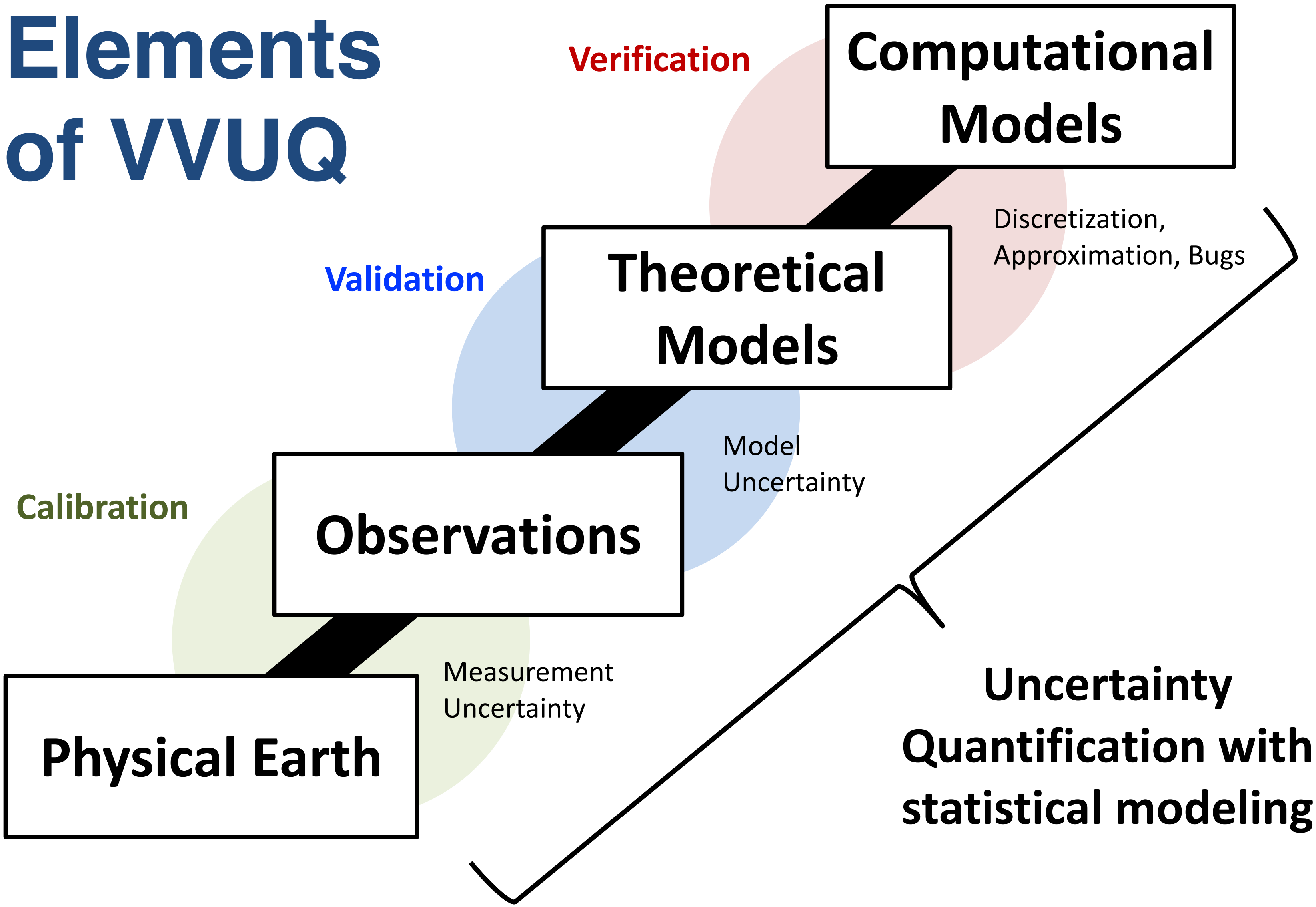

david.r.thompson@jpl.nasa.gov

Why is VVUQ important?

- Prerequisite for hypothesis testing and model comparison

david.r.thompson@jpl.nasa.gov

Why is VVUQ important?

- Prerequisite for hypothesis testing and model comparison
- Achieves a more complete understanding of the observation/retrieval system

david.r.thompson@jpl.nasa.gov

Why is VVUQ important?

- Prerequisite for hypothesis testing and model comparison
- Achieves a more complete understanding of the observation/retrieval system
- Enables data fusion across sensors, times, regions, atmospheres

david.r.thompson@jpl.nasa.gov

Why is VVUQ important?

- Prerequisite for hypothesis testing and model comparison
- Achieves a more complete understanding of the observation/retrieval system
- Enables data fusion across sensors, times, regions, atmospheres
- Provides accurate uncertainty estimates for policymakers and downstream analysts

david.r.thompson@jpl.nasa.gov

Why is VVUQ important?

- It predicts future instrument performance to validate instrument requirements

david.r.thompson@jpl.nasa.gov

Example: OCO-2 Mission

- Level 2 product is the column-averaged dry air mole fraction for CO_2 (X_{CO2})

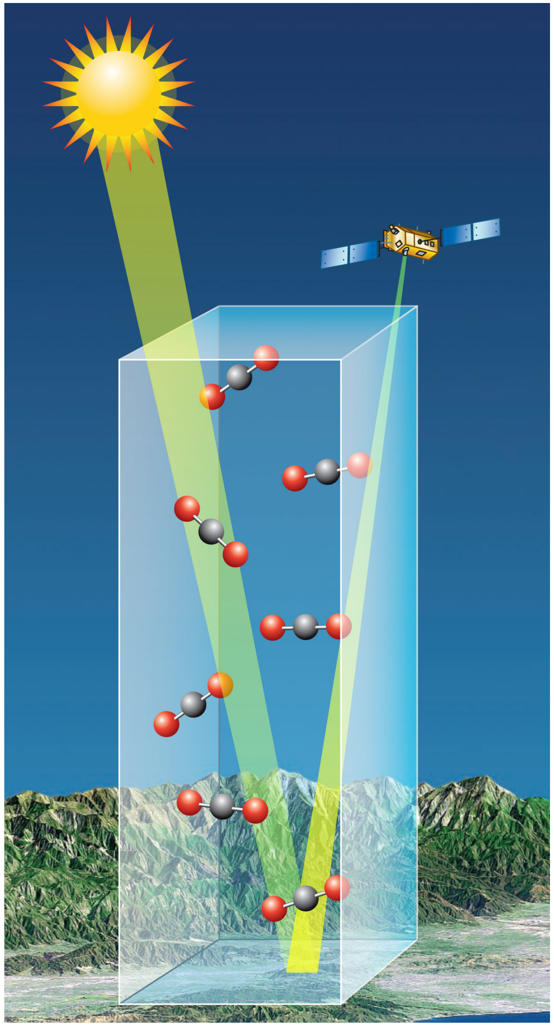

Image: NASA/JPL

Example: OCO-2 Mission

- Level 2 product is the column-averaged dry air mole fraction for CO_2 (X_{CO2})
- The retrieval algorithm finds a maximum a posteriori (MAP) solution within an optimal estimation (OE) framework
  - Physics-based radiative transfer model
  - Input is calibrated radiances and meteorology

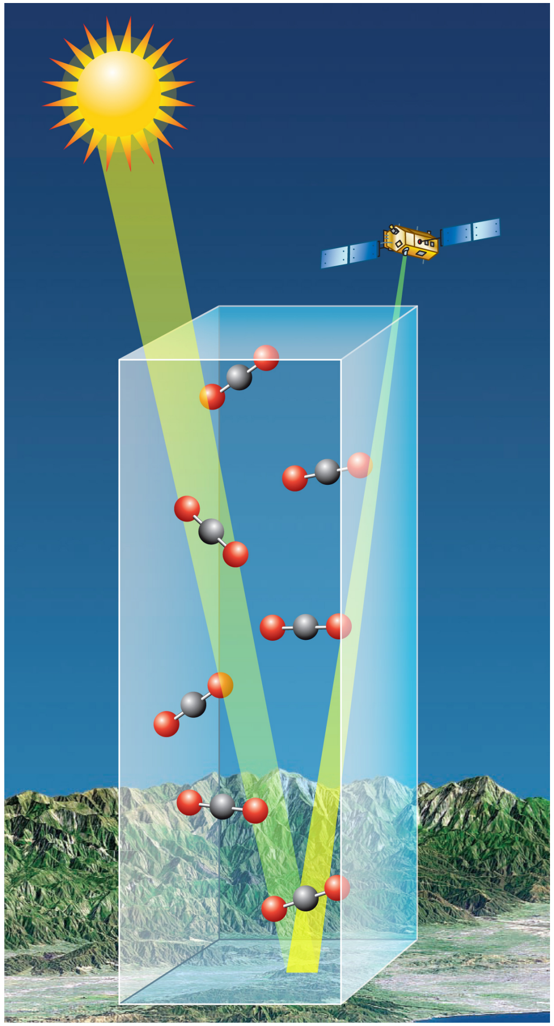

Image: NASA/JPL

david.r.thompson@jpl.nasa.gov

Example: OCO-2 Mission

- **Validation** compares retrieved X_{CO2} to ground station measurements from the Total Column Carbon Observing Network (TCCON) throughout phase E

Example: OCO-2 Mission

- **Validation** compares retrieved X_{CO2} to ground station measurements from the Total Column Carbon Observing Network (TCCON) throughout phase E
- **Verification** uses software functional unit tests, end-to-end regression tests, and a forward-to-inverse tool

david.r.thompson@jpl.nasa.gov

Example: OCO-2 Mission

- **Validation** compares retrieved X_{CO2} to ground station measurements from the Total Column Carbon Observing Network (TCCON) throughout phase E
- **Verification** uses software functional unit tests, end-to-end regression tests, and a forward-to-inverse tool
- **Uncertainty Quantification** uses the OE framework for estimating posterior uncertainty from measurement error and a priori knowledge of quantity of interest.
  - Linear sensitivity studies
  - Monte Carlo simulation studies of operational or alternative retrieval configurations

Agenda

- Motivation and Elements of VVUQ
- Example: The OCO-2 Mission
- VVUQ for imaging spectroscopy
- UQ for requirements definition

david.r.thompson@jpl.nasa.gov

Imaging spectroscopy case study

[Thompson et al., *Remote Sensing of Environment* 2018]

- AVIRIS-NG remote data
- In-situ Reagan sunphotometers
- In-situ ASD spectrometers
- Six validation sites at three locations
- Diverse surfaces, altitudes and solar illuminations

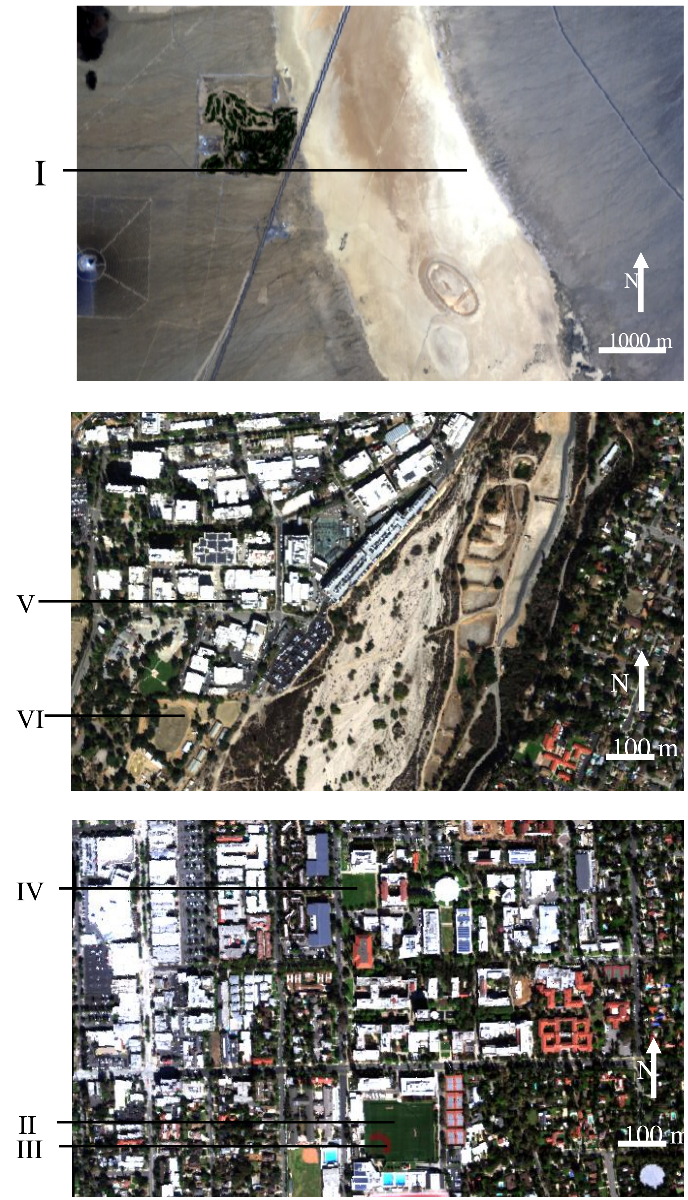

Iterative Maximum A Posteriori

[Thompson et al., *Remote Sensing of Environment* 2018]

Optimal estimation: A statistically-rigorous inversion incorporates prior and measurement distributions across the full spectral range. Enables rigorous uncertainty accounting.

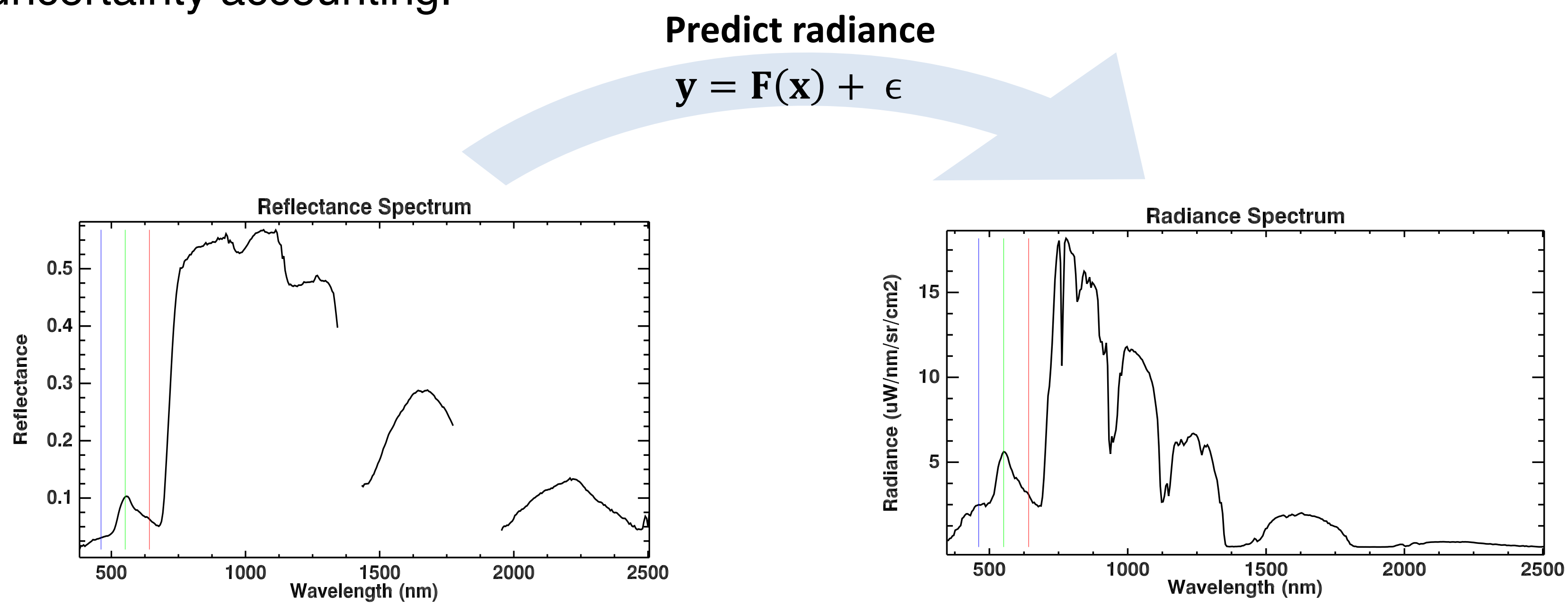

Iterative Maximum A Posteriori

[Thompson et al., *Remote Sensing of Environment* 2018]

Optimal estimation: A statistically-rigorous inversion incorporates prior and measurement distributions across the full spectral range. Enables rigorous uncertainty accounting.

Predict radiance

$$\mathbf{y} = \mathbf{F}(\mathbf{x}) + \epsilon$$

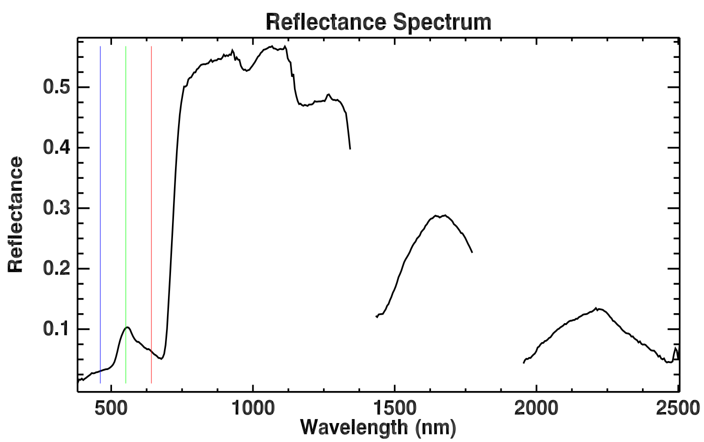

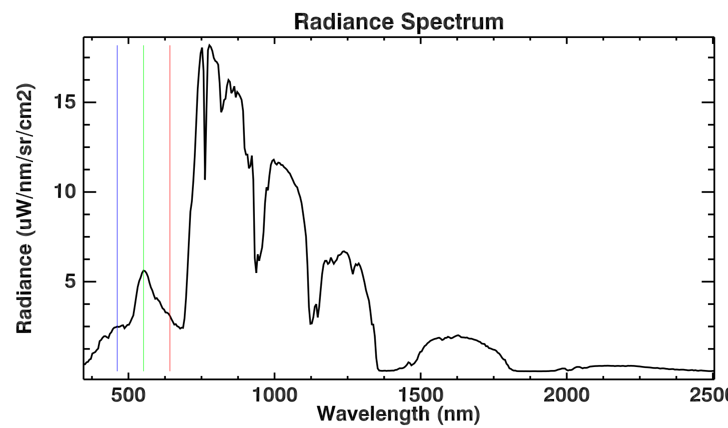

Optimize state vector

$$\underbrace{\chi^2(\mathbf{x})}_{\text{Cost}} = \underbrace{(\mathbf{F}(\mathbf{x}) - \mathbf{y})^{\mathbf{T}}\, \mathbf{S}_{\epsilon}^{-1}\, (\mathbf{F}(\mathbf{x}) - \mathbf{y})}_{\text{Model match to measurement}} + \underbrace{(\mathbf{x} - \mathbf{x}_{\mathbf{a}})^{\mathbf{T}}\, \mathbf{S}_{\mathbf{a}}^{-1}\, (\mathbf{x} - \mathbf{x}_{\mathbf{a}})}_{\text{Bayesian prior}}$$

Cost — Model match to measurement — Bayesian prior

david.r.thompson@jpl.nasa.gov

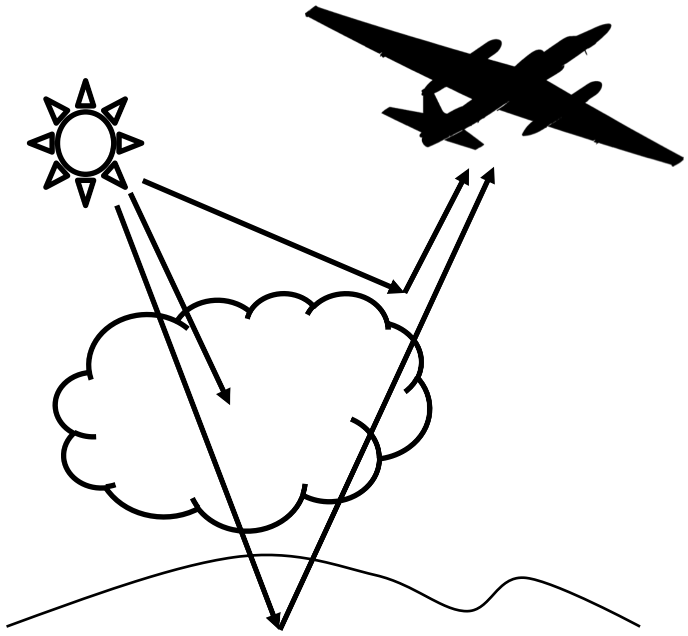

Instrument: AVIRIS-NG

Atmosphere: MODTRAN 6.0 RTM

Model components

Surface: Multi-component Multivariate Gaussians

david.r.thompson@jpl.nasa.gov

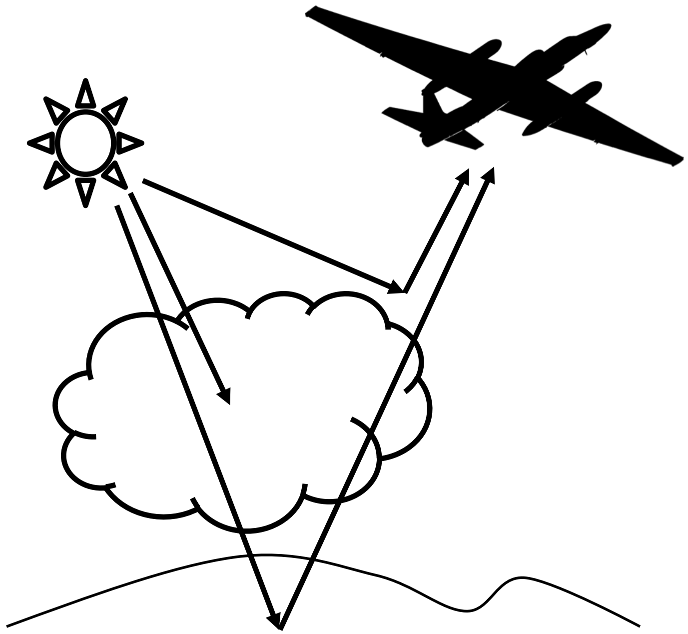

Instrument: AVIRIS-NG

- Instrument model with Wavelength- and signal-dependent SNR
- Photon shot & read noise

Atmosphere: MODTRAN 6.0 RTM

- DISORT MS, Correlated-k
- Rural aerosol model

Model components

Pre-defined

Surface: Multi-component Multivariate Gaussians

david.r.thompson@jpl.nasa.gov

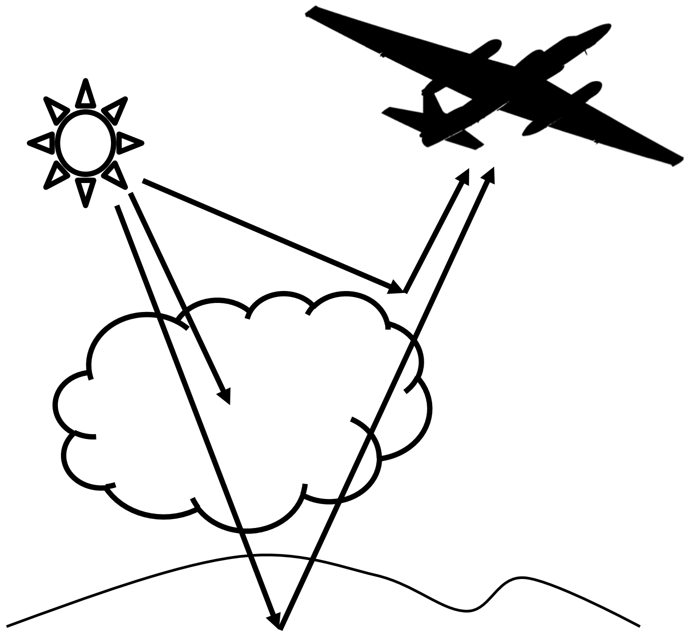

Model components

Pre-defined

Statistical, fit to data

Instrument: AVIRIS-NG

- Instrument model with Wavelength- and signal-dependent SNR
- Photon shot & read noise
- Uncorrelated calibration uncertainty
- Systematic calibration / RT uncertainty

Atmosphere: MODTRAN 6.0 RTM

- DISORT MS, Correlated-k
- Rural aerosol model
- broad prior uncertainties
- Unmodeled unknowns, including H_2O absorption coefficients

Surface: Multi-component Multivariate Gaussians

- Prior based on universal library, highly regularized to permit accurate retrieval of arbitrary shapes

david.r.thompson@jpl.nasa.gov

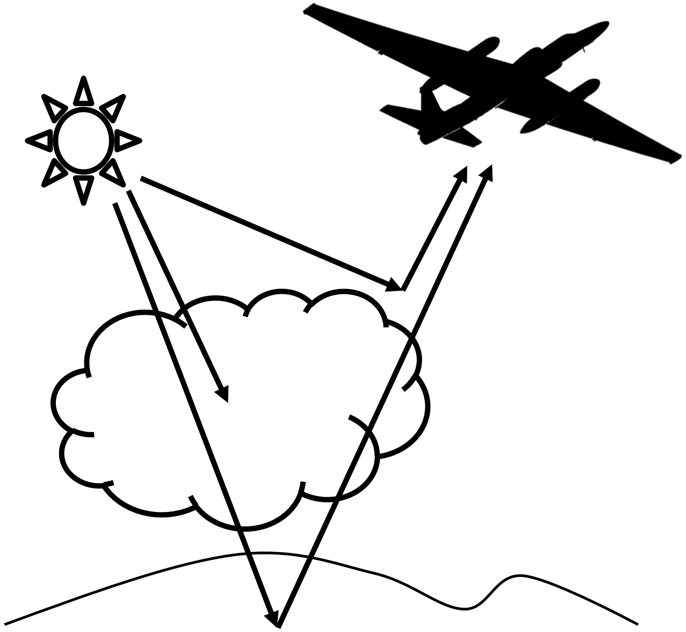

Model components

Pre-defined
Statistical, fit to data
Retrieved in the inversion

Instrument: AVIRIS-NG
- Instrument model with Wavelength- and signal-dependent SNR
- Photon shot & read noise
- Uncorrelated calibration uncertainty
- Systematic calibration / RT uncertainty

Atmosphere: MODTRAN 6.0 RTM
- DISORT MS, Correlated-k
- Rural aerosol model
- broad prior uncertainties
- Unmodeled unknowns, including H_2O absorption coefficients
- H_2O, AOD retrieved

Surface: Multi-component Multivariate Gaussians
- Prior based on universal library, highly regularized to permit accurate retrieval of arbitrary shapes
- Reflectance estimated independently in every channel

david.r.thompson@jpl.nasa.gov

Radiance model vs. measurement

[Thompson et al., *Remote Sensing of Environment* 2018]

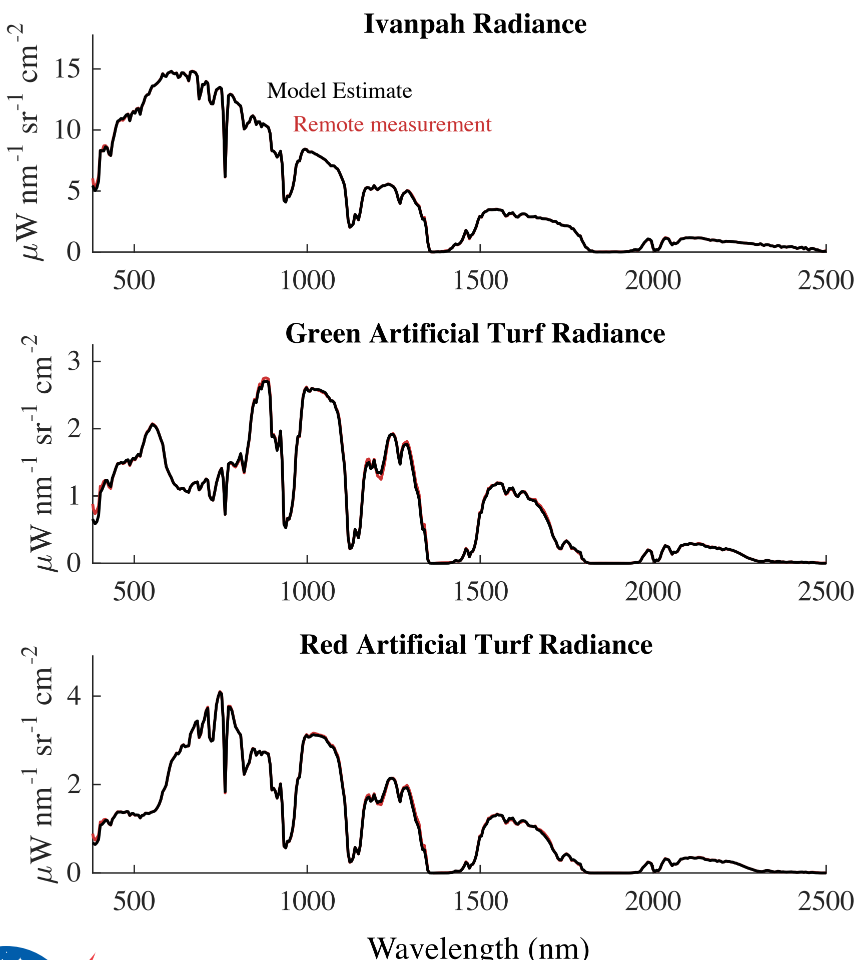

david.r.thompson@jpl.nasa.gov

Reflectance estimate vs. in situ

[Thompson et al., *Remote Sensing of Environment* 2018]

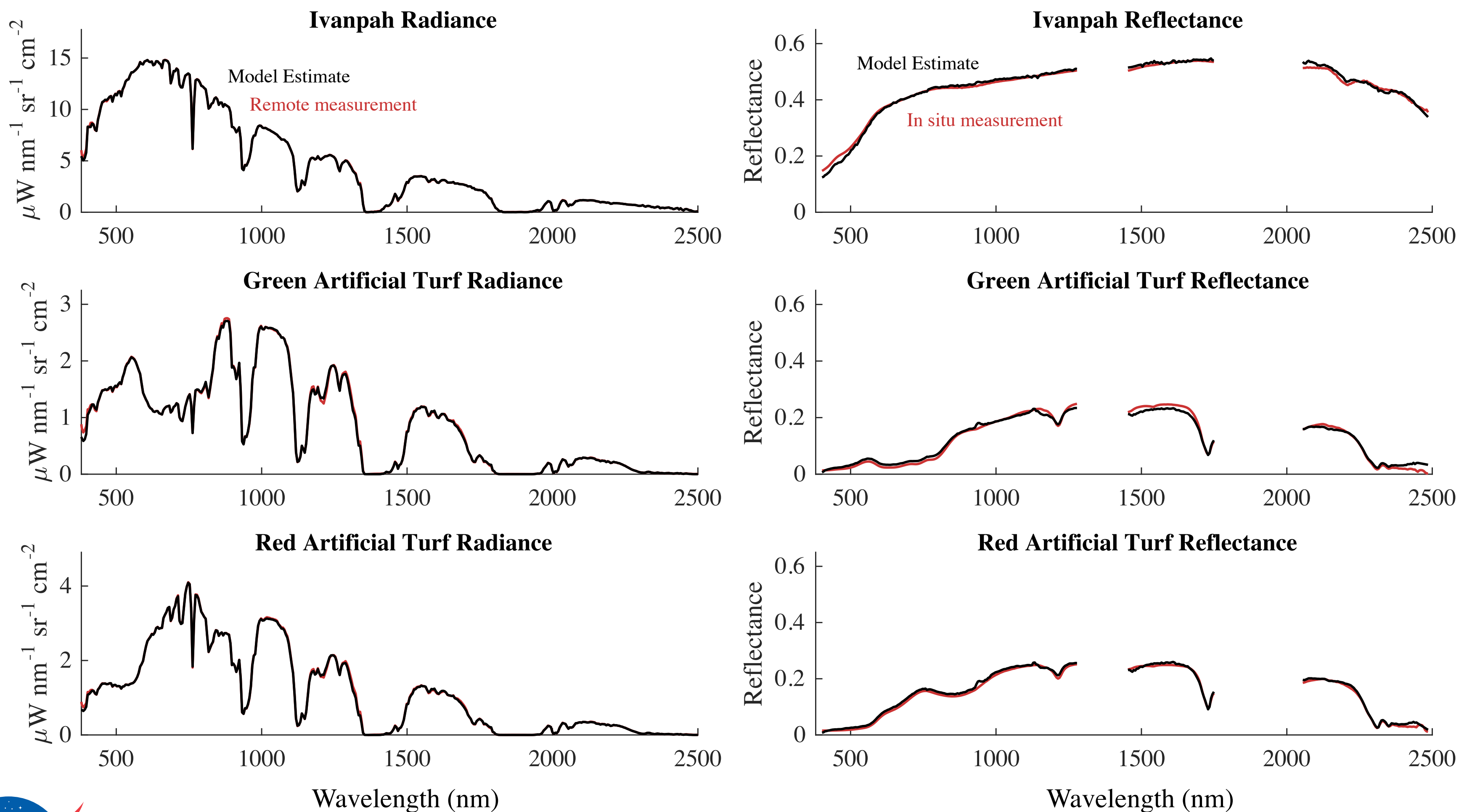

Posterior uncertainty compared to actual discrepancies

[Thompson et al., *Remote Sensing of Environment* 2018]

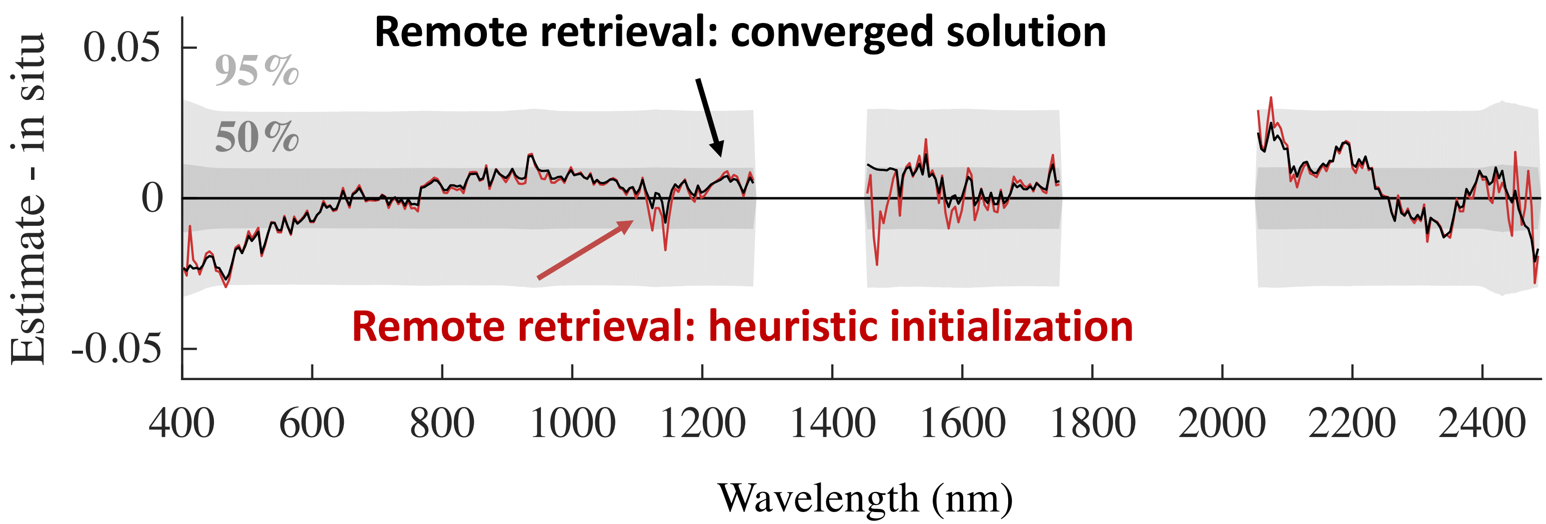

david.r.thompson@jpl.nasa.gov

Linear sensitivity analysis vs. Markov Chain Monte Carlo

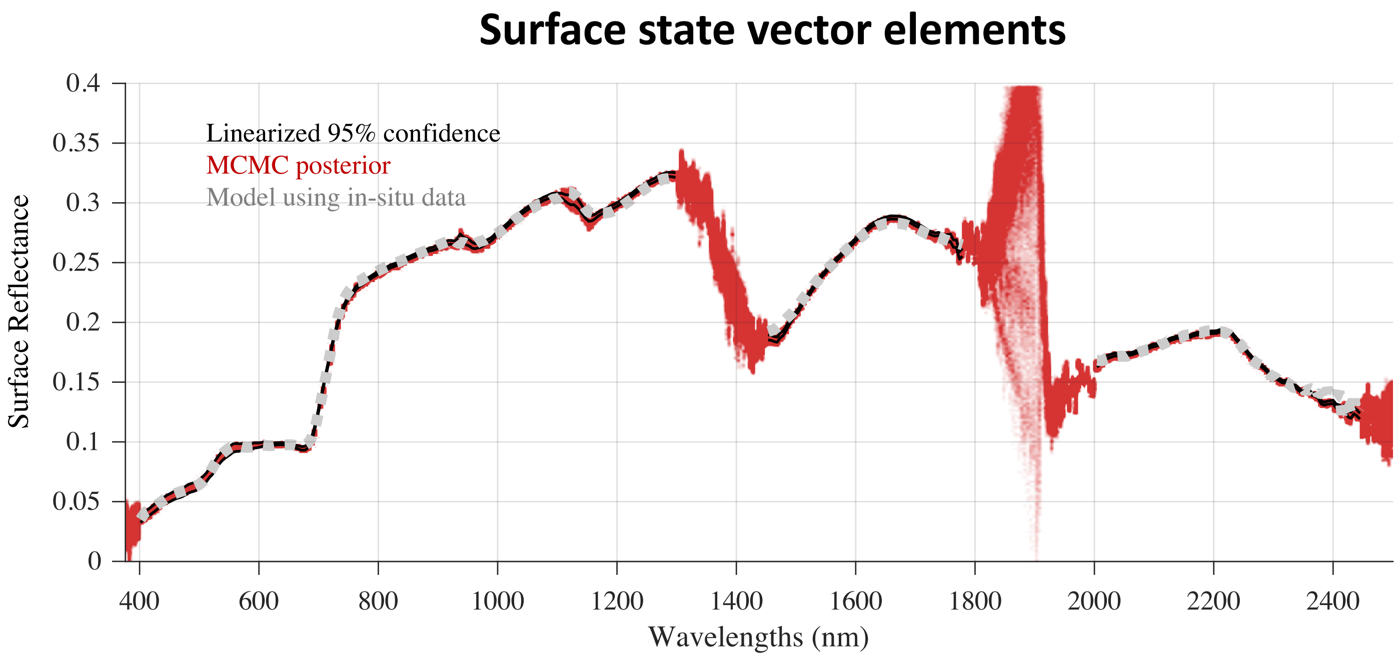

AVIRIS-NG at Karnataka, India 10 January 2016, Courtesy Manoj Mishra (ISRO/SAC)

Linear sensitivity analysis vs. Markov Chain Monte Carlo

Atmospheric state vector elements

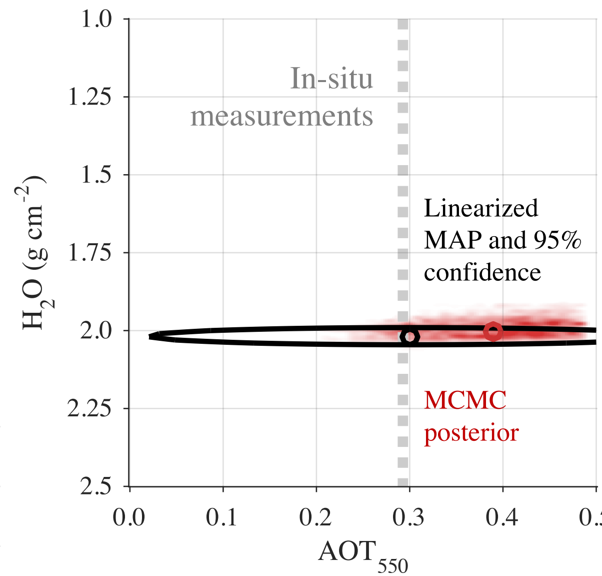

Surface state vector elements

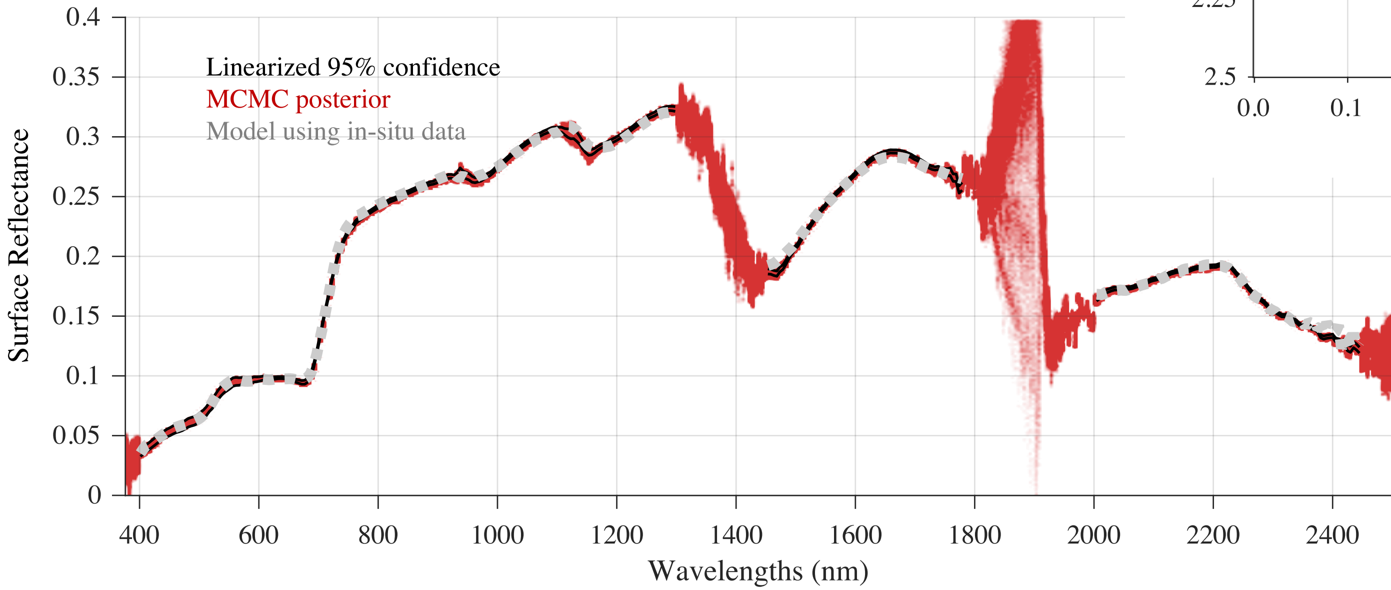

AVIRIS-NG at Karnataka, India 10 January 2016, Courtesy Manoj Mishra (ISRO/SAC)

david.r.thompson@jpl.nasa.gov

Agenda

- Motivation and Elements of VVUQ
- Example: The OCO-2 Mission
- VVUQ for imaging spectroscopy
- UQ for requirements definition

Forward models predict instrument performance

1. Forward-simulate observations under specific conditions
2. Perform retrievals and compare against the truth

david.r.thompson@jpl.nasa.gov

Forward models predict instrument performance

1. Forward-simulate observations under specific conditions
2. Perform retrievals and compare against the truth

Example: For what aerosol optical depths can AVIRIS-NG achieve a required reflectance accuracy (**spectral angle < 0.03**) for the Pasadena scene?

david.r.thompson@jpl.nasa.gov

Forward models predict instrument performance

1. Forward-simulate observations under specific conditions
2. Perform retrievals and compare against the truth

Example: For what aerosol optical depths can AVIRIS-NG achieve a required reflectance accuracy (**spectral angle < 0.03**) for the Pasadena scene?

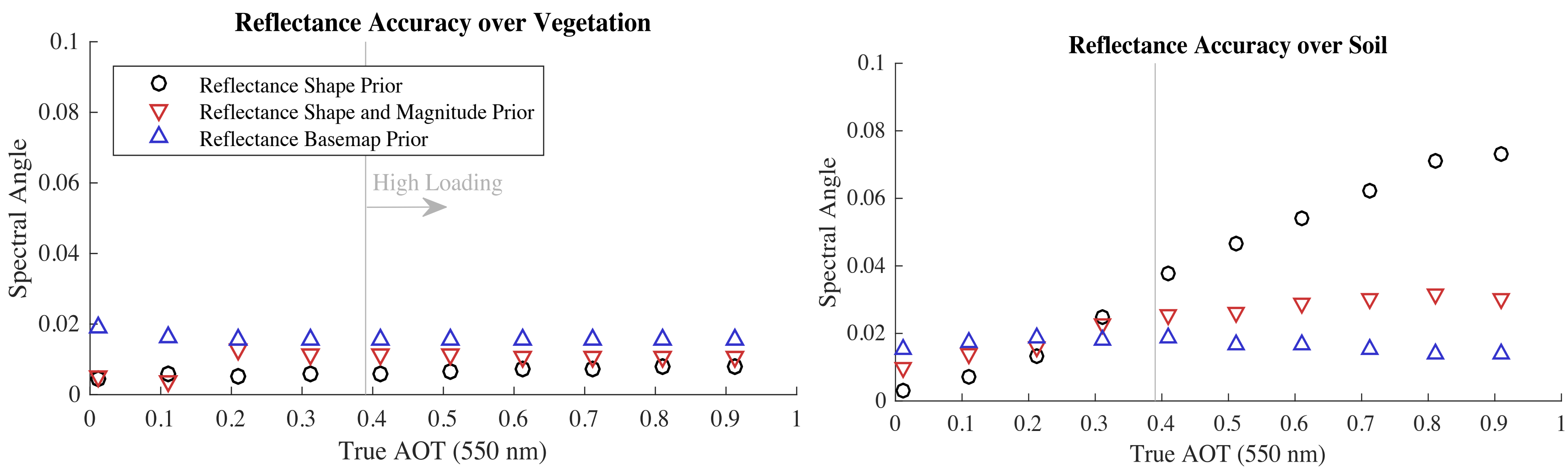

[Graphic from Thompson et al., *Remote Sensing of Environment* 2018]

Forward models predict instrument performance

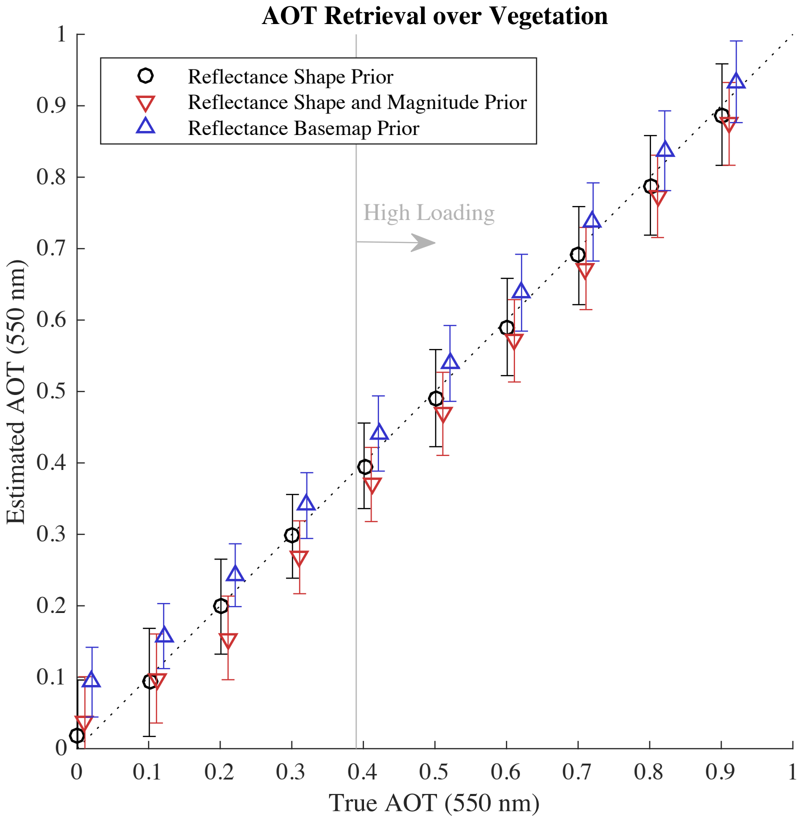

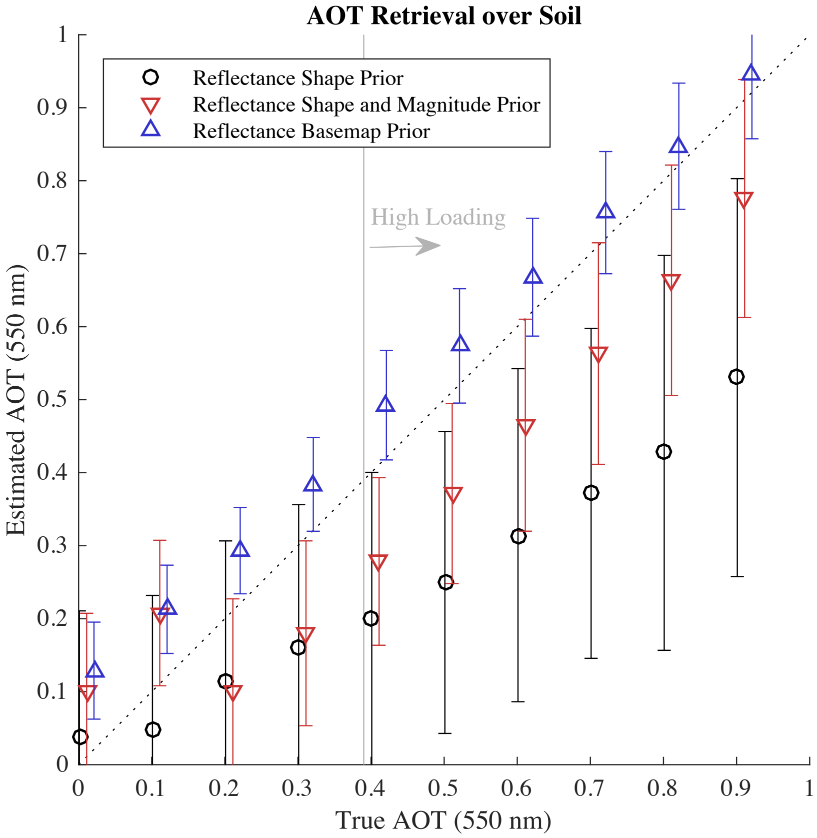

[Graphic from Thompson et al., *Remote Sensing of Environment* 2018]

david.r.thompson@jpl.nasa.gov

Quantifying Science Yield

Basic

Refined

1. **Instrument Spec -** "Back of Napkin" based on analogy to prior investigations, spectral/spatial coverage, resolution

david.r.thompson@jpl.nasa.gov

Quantifying Science Yield

Basic

1. **Instrument Spec -** "Back of Napkin" based on analogy to prior investigations, spectral/spatial coverage, resolution

2. **Retrieval uncertainty for representative observations**

Refined

david.r.thompson@jpl.nasa.gov

Quantifying Science Yield

Basic

1. **Instrument Spec -** "Back of Napkin" based on analogy to prior investigations, spectral/spatial coverage, resolution

2. **Retrieval uncertainty for representative observations**

3. **Retrieval uncertainty for realistic distribution of observations**

Refined

david.r.thompson@jpl.nasa.gov

Quantifying Science Yield

Basic

Refined

1. **Instrument Spec -** "Back of Napkin" based on analogy to prior investigations, spectral/spatial coverage, resolution
2. **Retrieval uncertainty for representative observations**
3. **Retrieval uncertainty for realistic distribution of observations**
4. **Posterior uncertainty in main objective, under a realistic simulated mission (full OSSE)**

david.r.thompson@jpl.nasa.gov

SBG AGU Session

Abstract ID# 416875: A Floating Vegetation Index (FVI) formed with three near-IR channels in the 1.0 – 1.24 micron spectral range for detecting vegetation floating over water surfaces
Abstract ID# 439379: Aerosol atmospheric correction of hyperspectral image data collected in India
Abstract ID# 424185: Airborne Imaging Spectroscopy of Coral Reef Condition
Abstract ID# 369132: (Invited) Change Temporary Title and Complete Invited Paper 369132
Abstract ID# 370344: Close-Range Hyperspectral Imaging of Dynamic Vegetation Communities in a High Arctic Tundra Ecosystem
Abstract ID# 399601: Compact Hyperspectral Prism Spectrometer: Recent Flight Campaign and Applications to the Future of Sustainable Land Imaging
Abstract ID# 370208: Constraining physically-based climate modeling with snow spectroscopic measurements from the Surface Biology and Geology concept
Abstract ID# 406039: DESIS on ISS, first results from commissioning phase
Abstract ID# 360017: Detection & Instrument Characterization Using Spatial Statistical Models
Abstract ID# 441816: Determining the Photosynthetic fAPARchl Canopy Fraction with EO-1 Hyperion Images
Abstract ID# 380013: Drought Response of Urban Vegetation using Airborne Imaging Spectroscopy
Abstract ID# 400233: Enabling a Threshold-Selection Algorithm for Excising Cloud-Contaminated Data Onboard Orbital Imaging Spectrometers
Abstract ID# 420163: Fast and reliable gas path-concentration inversion for thermal InfraRed (IR) hyperspectral imaging data obtained from downward looking sensors.
Abstract ID# 396086: Flight Research Techniques That Bring Results Using NASA Armstrong Airborne Science ER-2, G3, and DC-8 Aircraft
Abstract ID# 395924: High spectral resolution datasets of in situ aquatic inherent and apparent optical properties
Abstract ID# 381643: High-throughput phenotyping of photosynthetic capacities: an ensemble approach based on multiple machine learning models
Abstract ID# 426594: Hyperspectral based Mapping of Hydrothermal Altered Minerals using AVIRIS-NG Data and Machine Learning Algorithms in Hutti-Maski Gold Deposit Region, India
Abstract ID# 404173: Hyperspectral Imaging Airborne Campaign (VNIR-SWIR-TIR) in South Africa – Mineral resources applications
Abstract ID# 415403: Hyperspectral measurements identify contrasting physiological effects of different pathogens in crops
Abstract ID# 435577: Hyperspectral Remote Sensing of Optically Shallow Waters: Radiometric Challenges and Strategies
Abstract ID# 450761: HypMap: a web-based application for hyperspectral data visualization
Abstract ID# 423338: Imaging Spectroscopy Applications for Assessing Wetland Vegetation Distributions and Coastal Resiliency in Louisiana
Abstract ID# 449442: Improving Accuracy of Salt Marsh Aboveground Biomass using High-Spatial Resolution, Multi-View Hyperspectral Imaging Systems
Abstract ID# 368996: (Invited) Insights from the Decadal Survey process: Advancing global thermal infrared imaging for improved surface biology and geology science
Abstract ID# 382667: Inversion Strategies to Retrieve Snow Albedo and Temperature from Spectrometers and Multispectral Sensors
Abstract ID# 400279: Mapping REE-mineralogy using AVIRIS-NG hyperspectral data at the Mountain Pass Mine, California USA
Abstract ID# 447361: Mapping Vegetation Cover Fractions using Brightness Corrected Hyperspectral Image Mosaics and Machine Learning Regression
Abstract ID# 444240: Neural Network Radiative Transfer for Imaging Spectroscopy
Abstract ID# 382341: Prioritizing aquatic science and applications needs in the Chesapeake Bay for a space-borne hyperspectral mission
Abstract ID# 403352: Quantifying Methane Leak Emissions by Fused Airborne Imaging Spectroscopy with in situ Surface Mobile and Airborne Observations of a California Producing Oil Field
Abstract ID# 368449: Quantifying the Information Content of Global Imaging Spectroscopy
Abstract ID# 422126: Remote Detection of Plant Drought Stress Using Airborne Imaging Spectrometer Data Over a Three Year Period of Progressive Drought
Abstract ID# 455355: Seasonal and diurnal drone and ground-based thermal, multispectral and hyperspectral imaging to quantify responses of California oak woodland productivity and evapotranspiration …
Abstract ID# 433755: Soil Color: the Spectral Soil Line
Abstract ID# 440822: Spatio-temporal Variations of CDOM in Shallow Inland Waters from a Semi-analytical Inversion of Landsat-8
Abstract ID# 408667: Spatiotemporal Rice Phenology and Imaging Spectroscopy
Abstract ID# 410193: Structure and Function of Ecosystems – a Smallsat Compliment to SBG
Abstract ID# 370934: Surface-independent Aerosol Retrieval from Hyperspectral Imagery
Abstract ID# 436010: The Impending Flood of Imaging Spectroscopy Data: Is Ecosystem Science Ready?
Abstract ID# 393836: Thermal footprints preceding volcanic eruptions
Abstract ID# 456505: Thermal Infrared Science and Applications from HyTES and ECOSTRESS in Support of Surface Biology and Geology Science
Abstract ID# 408167: Using AVIRIS-NG Imagery to Map Agricultural Systems with Binary Classifiers and Limited Field Data
Abstract ID# 449208: Using Hyperspectral Imagery and Vegetation Indices to Predict Tree Mortality in a Northeastern American Forest
Abstract ID# 360859: Utilizing Spectral Imagery to Examine High Latitude Ecosystem Function and Diversity
Abstract ID# 413454: Visible/Shortwave and Thermal Infrared Measurements at Cuprite, Nevada: Complementary or Corroborating?

Thanks!

NASA Earth Science Division and the HyspIRI preparatory campaign

The AVIRIS-NG Team, including Sarah Lundeen, Brian D. Bue, Winston Olson-Duvall, John Chapman, and others

JPL Research and Technology Development program

NASA Program NNH16ZDA001N-AVRSN, “Utilization of Airborne Visible/Infrared Imaging Spectrometer – Next Generation Data from an Airborne Campaign in India.” Program manager Woody Turner

Backup

Posterior Error decomposition

$$\hat{\mathbf{S}} = \mathbf{G}\mathbf{S}_{\epsilon}\mathbf{G}^{T} + (\mathbf{I} - \mathbf{A})\mathbf{S}_{a}(\mathbf{I} - \mathbf{A})^{T}$$
$$= \mathbf{S}_{n} + \mathbf{S}_{m}$$

Uncertainty due to observation noise

Uncertainty due to resolution of the retrieval

david.r.thompson@jpl.nasa.gov

Posterior Error decomposition

$$\hat{\mathbf{S}} = \mathbf{G}\mathbf{S}_\epsilon\mathbf{G}^T + (\mathbf{I}-\mathbf{A})\mathbf{S}_a(\mathbf{I}-\mathbf{A})^T$$

$$= \mathbf{S}_n + \mathbf{S}_m$$

Uncertainty due to observation noise

Uncertainty due to resolution of the retrieval

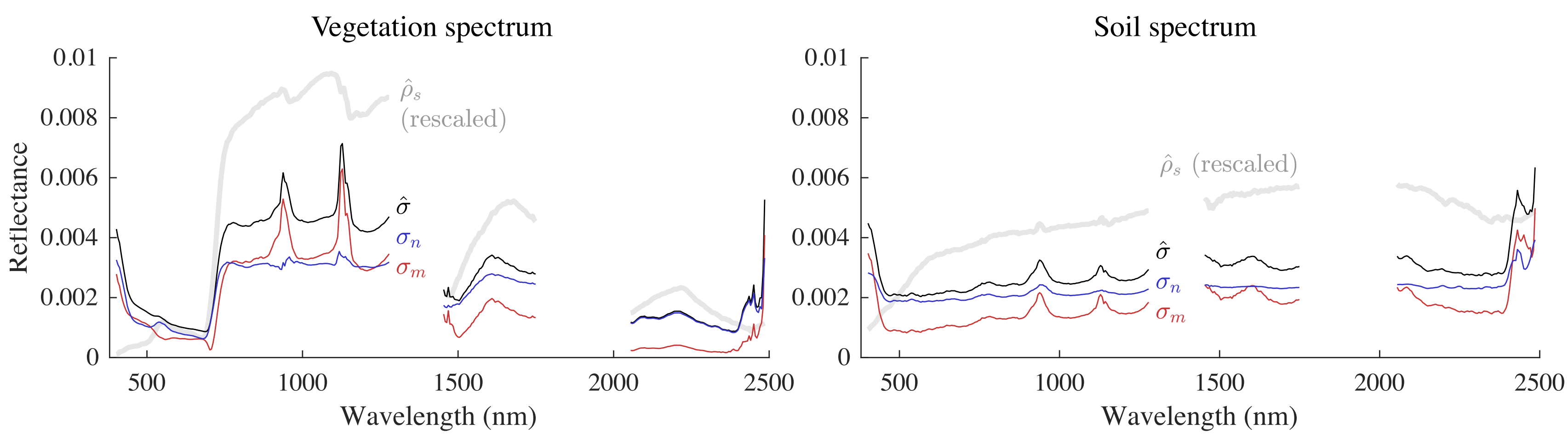

[Graphic from Thompson et al., *Remote Sensing of Environment* 2018]

david.r.thompson@jpl.nasa.gov